Mn K-edge XANES spectra of manganites measured by K_β emission.

J. García,[a]* M. C. Sánchez,[a] G. Subías,[a] J. Blasco[a] and M. G. Proietti[a]

[a]*Instituto de Ciencia de Materiales de Aragón, C.S.I.C.-Universidad de Zaragoza, CL Pedro Cerbuna 12, 50009 Zaragoza, Spain.*
Email:jgr@posta.unizar.es

The electronic state of Mn atoms in mixed valence manganites has been studied by means of X-ray absorption spectroscopy at the Mn K-edge. Higher resolution than in conventional measurements has been achieved by measuring the Mn K_β fluorescence line.
We have found a unique resonance at the edge in the XANES spectra of intermediate composition $RE_{1-x}Ca_xMnO_3$ samples. The features of these XANES spectra do not depend on small changes in the local structure around the Mn atom. However, the spectra of the intermediate composition samples can not be reproduced by a linear combination of $REMnO_3$ and $CaMnO_3$ spectra. Accordingly, the electronic state of Mn atoms in these compounds can not be considered as a mixture of Mn^{3+} and Mn^{4+} pure states.

Keywords: Giant magnetoresistance, charge-ordering, XANES

1. Introduction

Perovskites $RE_{1-x}D_xMnO_3$ (RE= Rare earth atom, D= divalent atom as Ca, Sr) show a very rich phenomenology, depending on the RE^{3+}/D^{2+} content ratio, RE^{3+}/D^{2+} average ionic size and RE^{3+}/D^{2+} size mismatch. In $La_{1-x}Ca_xMnO_3$ series, a metal-insulator transition coupled to a ferromagnetic ordering has been found for $0.2 \leq x \leq 0.5$. Different kinds of electronic localisation and spin ordering phenomena have been observed for $x<0.2$ and $x \geq 0.5$, including the so-called "charge-ordered" states (Chen *et al.*, 1993; Kuwahara *et al.*, 1995). The magnetic ground state for the latter composition range is antiferromagnetic but different types of magnetic structures are found depending on the x value. The substitution of La by other RE with smaller ion size reduces the strength of the ferromagnetic interactions and, consequently, expands the composition range for the charge ordered structures (Coey *et al.*, 1999).
Generally, mixed valence manganites have been described considering an ionic model, i.e. as $RE_{1-x}D_xMn^{3+}{}_{1-x}Mn^{4+}{}_xO_3$. In this way, it is thought that charge-ordering states arise from the localisation of e_g electrons on Mn^{3+} ions and that these ions are periodically ordered in the lattice to minimize the Coulomb repulsion. On the other hand, thermal activated hopping between adjacent Mn atoms is proposed for the semiconducting paramagnetic phase.
The study of the valence state of the manganese atoms in mixed valence perovskites has been the subject of several works; i) thermoelectric power experiments indicate the presence of more charge carriers than those expected from the doping ratio (Hundley *et al.*, 1997). ii) Electronic paramagnetic resonance measurements show the absence of isolated Mn ions in 2+, 3+ or 4+ states (Oseroff *et al.*, 1996). iii) XPES and O K-edge X-ray absorption spectroscopy show a significant discrepancy between the weighted spectra obtained by linear combination of the end members and the experimental spectrum (Park *et al*, 1996). iv) a Mn K_β emission spectroscopy study by Tyson *et al.* (1999) has shown that the emission spectra for the doped samples can be well fitted by a linear superposition of the end member spectra, but the weight of each component does not coincide with the formal Mn^{3+}/Mn^{4+}.
One of the main goals of our research is the identification of the electronic state for the Mn atom in these perovskite compounds. In a previous publication, we have analysed the valence state of the Mn atoms by using the Mn K-edge XANES spectra (Subías *et al.*, 1997). Our attention was mainly focused on magnetoresistive samples, i.e., $RE_{1-x}D_xMnO_3$ compounds with $x \approx 0.33$. Our results showed that Mn does not fluctuate between 3+ and 4+ valence states. In this paper, we extend this study to the whole series. With this purpose we have performed experiments improving the resolution beyond the broadening produced by the core-hole lifetime. The spectra have been measured by recording the Mn K_β emission, using a high-resolution spectrometer.
We present XANES spectra at the Mn K-edge of $RE_{1-x}Ca_xMnO_3$ (RE= La, Tb, x=1, 1/3, 1/2, 2/3, and 0), $RE_{0.5}D_{0.5}MnO_3$ (RE = La, Tb, D = Sr, Ca) and $La_{0.5}Sr_{1.5}MnO_4$ samples by measuring both the total fluorescence yield intensity and the Mn K_β fluorescence intensity (Hämäläinen *et al.*, 1991).

2. Experimental

Samples were prepared by standard ceramic procedures or using a sol-gel method by the citrate route. The samples were characterised by means of X-ray powder diffraction, magnetic and electrical transport properties (Blasco *et al.*, 2000; Ibarra *et al.*, 1997). The experiments were performed at the beam-line ID26 of the E.S.R.F. in Grenoble. Mn K edge XANES spectra were recorded simultaneously, measuring the total fluorescence yield and analysing the K_β fluorescence line by means of a Rowland circle spectrometer based on a spherical bent Si (440) monochromator. K_β emission and total fluorescence spectra have been recorded simultaneously. XANES spectra have been recorded measuring the intensity of the K_β fluorescence line at the emission spectra peak.

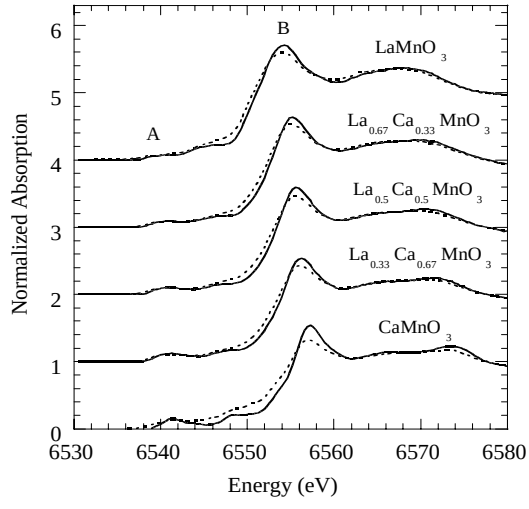

Figure 1
Normalized XANES spectra of $La_{1-x}Ca_xMnO_3$ series at room temperature recorded by Mn-K_β emission (continuous line) and total fluorescence yield (dashed line).

3. Results

Normalized XANES spectra for $La_{1-x}Ca_xMnO_3$ series at room temperature obtained by measuring both total fluorescence yield and Mn-K_β line fluorescence are compared in Fig. 1 (similar results were obtained for the $Tb_{1-x}Ca_xMnO_3$ series). We realized that the conventional (total fluorescence yield, TFY) spectra can be obtained from the K_β fluorescence spectra by a convolution with a Lorentzian function of about 0.8 eV width. The main difference is restricted to a feature in the $CaMnO_3$ spectrum (A_1 pre-peak of Fig 4, shown below). In this case, the sensitivity of the K_β fluorescence line to the spin state could be responsible for this discrepancy. All the other features of the $CaMnO_3$ spectrum and of the other spectra are present in both measurement modes.

The spectral line shapes are similar for all samples. They show a pre-edge structure (denoted as A in Fig 1) and a main resonance at the edge, characteristic of the Mn in octahedral coordination (denoted as B in Fig.1). The first pre-edge peak is located at about 10 eV below the inflection point and its intensity grows up significantly upon increasing the formal Mn^{4+} content. The main difference among the spectra arises from the chemical shift. The shift is nearly linear with the formal Mn valence state and it reaches a value of about 4.5 eV between $REMnO_3$ and $CaMnO_3$. The spectral differences beyond the absorption edge are due to small changes in the local structure among the samples.

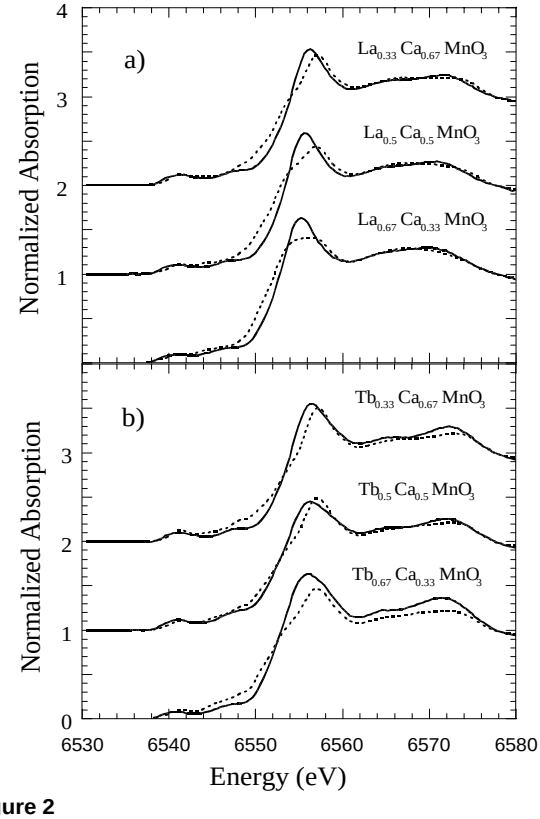

Figure 2
Comparison between the normalized high-resolution XANES spectra of $La_{1-x}Ca_xMnO_3$ (panel a) and $Tb_{1-x}Ca_xMnO_3$ (panel b) series (continuous line) and the spectra obtained by the averaged addition of the end members compounds spectra (dashed line).

In order to determine if the XANES spectra of $RE_{1-x}Ca_xMnO_3$ samples can be described in terms of a bimodal distribution of Mn^{3+} and Mn^{4+} ions, we have compared the XANES spectra of doped compounds to the averaged sum of the end-members spectra, i.e. (1-x) $REMnO_3$ + x $CaMnO_3$. These comparisons are shown in Fig 2. Although the edge position is reasonably well reproduced, strong differences between calculated and experimental spectra are obtained for all the samples. In particular, the experimental edge is sharper and the two main structures displayed in the calculated spectra are absent in the experimental ones.

It is well known that the shape of the XANES spectrum also depends on the particular local structure of the photoabsorbing atom. Consequently, it can be argued that the above analysis could be non-conclusive. In order to extract the common experimental features for all the samples, independently of small variations in the local structure, we have also measured the XANES spectra of different $RE_{0.5}Ca(Sr)_{0.5}MnO_3$ samples and of the $La_{0.5}Sr_{1.5}MnO_4$ compound. Our aim was to check how the XANES spectrum is affected by small changes in the local structure. In this way, we studied samples with different rare earth or divalent atoms keeping the ratio Mn^{3+}/Mn^{4+} =1. The results for several compounds are shown in Fig. 3. We observe similar spectra for all the samples. There are small variations in the intensity of the main resonance but the width is nearly equal for all of them. This is true even for the $La_{0.5}Sr_{1.5}MnO_4$ sample which has a different crystallographic structure. The main difference among the various spectra, to be related to the local structure, is located at energies above the main resonance. In conclusion, the main peak (denoted as B in Fig. 1) is the same for all these manganites and it can be used as a finger print of the Mn electronic state.

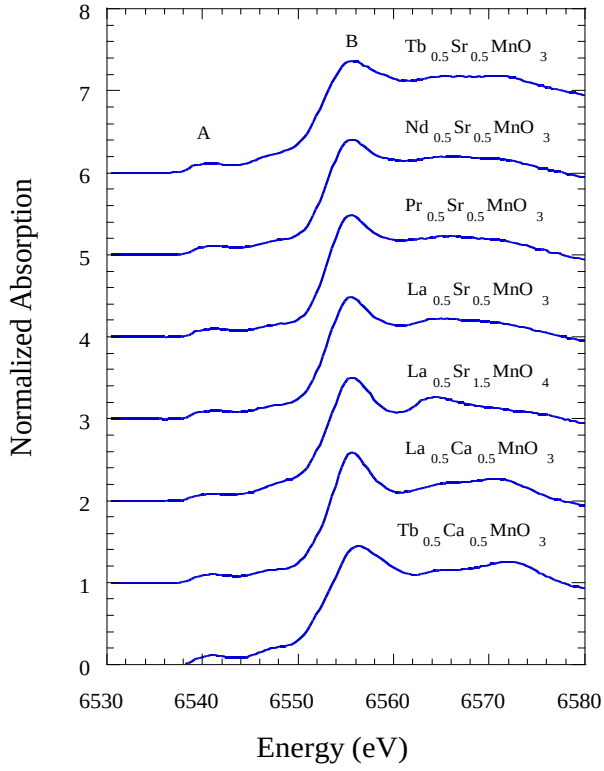

Figure3
Normalized high-resolution XANES spectra recorded by Mn-K_β fluorescence of $RE_{0.5}Sr_{0.5}MnO_3$ (RE=La, Tb, Nd, Pr), $RE_{0.5}Ca_{0.5}MnO_3$ (RE=La, Tb) and $La_{0.5}Sr_{1.5}MnO_4$ compounds.

Fig. 4 shows the pre-edge region of the K_β emission XANES spectra for the $La_{1-x}Ca_xMnO_3$ series. The resonance A is broad for doped samples whereas there is a clear splitting for $LaMnO_3$ (hereafter denoted as A_1 and A_2). The K_β emission spectrum of

$CaMnO_3$ only shows a peak whereas the TFY spectrum shows a splitting. This is the only discrepancy between both modes of measurement. The lack of the A_1 peak in the K_β emission spectra of $CaMnO_3$ indicates the majority spin character for this peak in this sample, i.e. this transition occurs mainly to states with spin parallel to the Mn 3d spin (Hämäläinem *et al.*, 1992). The rest of the samples show the same features in TFY and in K_β emission spectra. Consequently, the A_1 state of $LaMnO_3$ and of the doped samples does not seem to be sensitive to the spin. The splitting between A_1 and A_2 is 1.7 eV and 2.0 eV for $LaMnO_3$ and $CaMnO_3$ (only TFY spectrum) respectively. This splitting is around 1.3 eV for doped samples. Moreover, we note that the peak A_2 continuously shifts to higher energies as the average valence state of Mn atoms increases. On the other hand, the intensity of the pre-peaks grows up with the Ca content. This result suggests an increase of the covalence between Mn-3d and O-p empty states. It is worth to notice that the spectra of mixed valence compounds are very similar to each other, but quite different from those of the end-member samples. Therefore, the assumption of electronic transitions to the same band states for both, the mixed valence and the undoped compounds is difficult to reconcile with the experimental data.

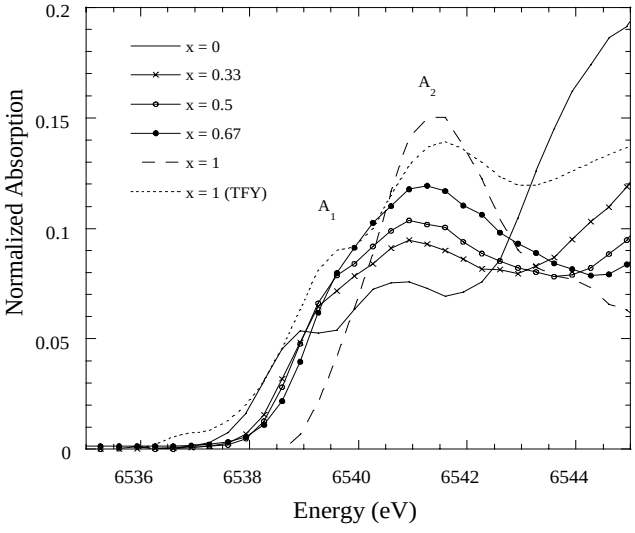

Figure 4
Pre-edge region of the high-resolution XANES spectra of $La_{1-x}Ca_xMnO_3$ series. Total fluorescence yield (TFY) of $CaMnO_3$ (continuous line) is also reported.

4. Discussion and conclusions

We have shown that XANES spectra of $RE_{1-x}Ca_xMnO_3$ samples can not be obtained by the averaged addition of the end-member's of the series spectra. However, it does not mean that all the Mn atoms are identical from a geometrical and electronic point of view. In order to check the sensitivity of our data to small differences between Mn atoms, we have also compared the experimental spectra of $RE_{1/2}Ca_{1/2}MnO_3$ with the averaged sum of $RE_{2/3}Ca_{1/3}MnO_3$ and $RE_{1/3}Ca_{2/3}MnO_3$ spectra. The agreement between the experiment and the calculated spectra is very good, indicating that both, the electronic state and the local structure of Mn atoms are very similar for all the doped samples with x values close to each other. This is true even for samples, the macroscopic behaviour of which, are completely different (we note that $Tb_{1/2}Ca_{1/2}MnO_3$ shows a charge-ordered state at room temperature but not $Tb_{2/3}Ca_{1/3}MnO_3$ or $Tb_{1/3}Ca_{2/3}MnO_3$). From this analysis, one can affirm that neither Mn^{3+} nor Mn^{4+} exist in the intermediate $RE_{1-x}Ca_xMnO_3$ compounds but the presence of non-equivalent Mn ions can not be discarded.

Recent X-ray resonant scattering experiments at the Mn K edge on $La_{0.5}Sr_{1.5}MnO_4$, $Pr_{0.5}Ca_{0.5}MnO_3$ and $Nd_{0.5}Sr_{0.5}MnO_3$ have been reported (Von Zimmerman *et al.*, 1999; Murakami *et al.*, 1998; Nakamura *et al.*, 1999), claiming for a real charge ordering in these samples. We have reanalysed and reinterpreted these data (García *et al.*, 2000) showing that no real charge ordering of Mn^{3+} and Mn^{4+} exists in these compounds. The experiments here reported, instead, demonstrate the existence of two kinds of Mn atoms with two different geometrical environments.

In conclusion, the electronic localisation in manganites (either in the paramagnetic phase or in the charge-ordered phase) has to be considered as an open question. The electronic localisation should be span over several Mn atoms. Therefore, a cluster localisation, giving rises to phase segregation, a molecular polarons or the presence of the conducting states with lower dimensionality, could explain the semiconducting behaviour.

We would like to thank ESRF for beam time granting, Dr. C. Gauthier, Dr. A. Solé and Dr. Dr. M. H. Krisch for their kind assistance in the experiment. This work has been supported by the Spanish C.I.C.Y.T. project n. MAT99-0847.

References

Blasco, J., Ritter, C., García, J., de Teresa, J. M., Pérez-Cacho, J. & Ibarra, M. R. (2000). *Phys. Rev. B.* **62**, 5609-5618.
Chen, C. H., Cheong, S.-W. & Cooper, A. S (1993). *Phys. Rev. Lett.* **71**, 2461-2464.
Coey, J. M. D., Viret, M. & Von Molnar, S. (1999). *Adv. Phys.* **48**, 167-293.
García, J. , Sánchez, M. C. , Subías, G., Blasco, J. & Proietti, M. G. (2000) to be published.
Hämäläinen, K., Kao, C. C., Hastings, J. B., Siddons, D. P., Berman, L.E., Stojanoff, V. & Cramer, S. P. (1992). *Phys. Rev. B* **46**, 14274-14277.
Hämäläinen, K., Siddons, D. P., Hastings, J. B. & Berman, L.E. (1991). *Phys. Rev. Lett.* **67**, 2850-2853.
Hundley, M. F. & Neumeier, J. J. (1997). *Phys. Rev. B* **55**, 11511-11515.
Ibarra, M. R., de Teresa, J. M., Blasco, J., Algarabel, P.A., Marquina, C., García, J., Stankiewitz, J. & Ritter, C. (1997). *Phys. Rev. B* **56**, 8252-8525.
Kuwahara, H., Tomioka, Y., Asamitsu, A., Morimoto, Y., & Tokura, Y. (1995) Science **270**, 961-963.
Murakami, Y., Kawada, H., Kawada, H., Tanaka, M., Arima, T., Moritomo, Y. & Tokura, Y. (1998). *Phys. Rev. Lett.* **80**, 1932-1935.
Nakamura, K., Arima, T., Nakazawa, A., Wakabayashi, Y. & Murakami, Y. (1999). *Phys. Rev. B* **60**, 2425-2428.
Oseroff, S. B., Torikachvili, M., Singley, J., Ali, S., Cheong, S-W. & Schultz, S. (1996). *Phys. Rev. B* **53**, 6521-6525.
Park, J. H., Chen, C. T., Cheong, S-W., Bao, W., Meigs, G., Chakairan, V. & Idzerda, Y. U. (1996). *Phys. Rev. Lett.***76**, 4215-4218.
Subías, G., García, J., Proietti, M. G. & Blasco, J. (1997) *Phys.Rev. B.* **56**, 8183-8191.
Tyson, T. A., Qian, Q., Kao, C. C., Rueff, J. P., deGroot, F. M. F., Croft, M., Cheong, S-W., Greenblatt, M., & Subramanian, M. A. (1999). *Phys. Rev. B* **60**, 4665-4674.
Zimmerman, V. M., Hill, J. P., Gibbs, D., Blume, M., Casa, D., Keimer, B., Murakami, Y., Tomioka, Y. & Tokura, Y. (1999). *Phys. Rev. Lett.* **83**, 4872-4875.